

Synthesis of Mn-Co-Ni Composite Electrode by Anodic and Cathodic Electrodeposition for Indirect Electro-oxidation of Phenol: Optimization of the Removal by Response Surface Methodology

Yamama A. Ahmed^{1*}, Rasha H. Salman¹

¹ Department of Chemical Engineering, College of Engineering, University of Baghdad, Baghdad, Iraq

* Corresponding author's e-mail: yamama.ahmed1507D@coeng.uobaghdad.edu.iq

ABSTRACT

In the present work, Response Surface Methodology (RSM) was utilized to optimize process variables and find the best circumstances for indirect electrochemical oxidation of mimicked wastewater to remove phenol contaminants using prepared ternary composite electrode. The electrodeposition process is used for the synthesis of a ternary composite electrode of Mn, Co, and Ni oxides. The selected concentrations of metal salts of these elements were 0.05, 0.1, and 1.5 M, with constant molar ratio, current density, and electrolysis time of 1:1:1, 25 mA/cm², and 2 h. Interestingly, the gathered Mn-Co-Ni oxides were deposited at both the anode and cathode. X-ray diffraction (XRD) and scanning electron microscopy (SEM) facilitated the qualitative characterization of surface structure and morphology of the accumulated oxides. The energy dispersive X-ray (EDX) provided a semi-quantitative analysis of deposit composition. The atomic force microscopy (AFM) apparatus quantified the roughness. We examined the efficiency of composite electrodes in coinciding with the removal of Chemical Oxygen Demand (COD) under current densities of 40, 60, and 80 mA/cm², pH values of 3, 4, and 5, and NaCl concentrations of 1, 1.5, 2 g/l. RSM covered the optimization of process parameters in conjunction with Central Composite Design (CCD). The COD represented the response function in the optimization procedure. The optimal current density, NaCl concentration, and pH magnitude were 80 mA/cm², 1.717 g/l, and 3, respectively. The efficiency of COD elimination of 99.925% attained after 1 hour of indirect electrochemical oxidation with an energy consumption of 152.380 kWh per kilogram of COD. The COD elimination model is significant based on the correlation coefficient (R^2) and F-values, and the experimental data fitted well to a second-order polynomial model with R^2 of 98.93%.

Keywords: Composite electrode, indirect electro-oxidation, phenol removal, response surface methodology, electrodeposition

INTRODUCTION

Electrochemical oxidation of organic substances is a promising method for treating wastewater. Phenols are a significant group of industrial contaminants that are highly dangerous in bioaccumulation circumstances, particularly in wastewater discharges [Massa et al., 2017; Adil Sabbar, 2019]. Conventional wastewater remediation approaches are ineffective in breaking down these molecules rather than their drawbacks regarding environment and energy consumption [Nady et al., 2017; Al-Yaqoobi et al., 2021]. Alternatively, electrochemical methods imply the conservation

of energy and protection of the ecosystem [Abbar and Alkurdi, 2021; Abbas and Abbas, 2022].

Electrodeposition is one of the most efficient electrochemical processes that utilize a direct current or pulsed electric field in an electrolyte solution where ions are deposited on the surfaces of electrodes [Tahmasebi et al., 2016; Kazazi, 2018]. The concentration of metal salts in the electrolyte impacts the morphology, crystallography, and orientation of deposits [Yan et al., 2020]. Thus, the electrochemical deposition strategy is a talented process to synthesize several deposits of metal oxides [Sayyed et al., 2019].

The removal efficiency of phenol pollutants strongly relies upon the applied metal oxides in wastewater treatment. For example, transition metal oxides reflect extraordinary performance in the full breakdown of phenolic molecules [Ibrahim and Salman, 2022]. Oxides of cobalt (Co), nickel (Ni), and manganese (Mn) elements have attracted extensive studies regarding wastewater remediation topics [Li et al., 2016; Sui et al., 2019; Jiráková et al., 2021; Jadhav et al., 2021]. They are tremendously used in single oxide route processes [Abbas and Abbas, 2019; Tegui Doumbi et al., 2021]. Nonetheless, assembling binary or ternary systems of these three compounds was rarely investigated in the related field of water treatment. Recently, a new study has competently prepared and examined such oxide systems. It introduced them as reasonable options for the reduction of undesired phenolic compounds [Ahmed and Salman, 2023]. The targeted elimination of phenol via single oxides of Mn attained 99.9% only after an electrolysis time of 5 hours [Abbas et al., 2016]. However, one hour was adequate to obtain similar removal with Mn/Co/Ni-oxides scenarios [Ahmed and Salman, 2023]. Formation of deposits presents either on the anode [Zhu et al., 2019; Chelladurai et al., 2020; Cysewska et al., 2020] or cathode [El Boraei and Ibrahim, 2019], while very few researchers reported deposition of oxides on both cathode and anode simultaneously [Abebe and Ujihara, 2022; Ahmed and Salman, 2023]. In our latest publication, we synthesized a Mn-Ni-Co oxide electrode via the electrodeposition technique. The process parameters involved a constant salt concentration of 0.1 M of these elements and different current densities of 20, 25, 30, and 35 mA/cm². The effect of current density on the preparation electrodes was investigated and the performance of the prepared anode and cathode in indirect electrooxidation of phenol in specified conditions was studied. More details regarding the preparation and removal efficiency of the ternary oxide electrode of Mn-Ni-Co are present in our recent publication [Ahmed and Salman, 2023].

The response surface technique is one of the fundamental multivariate strategies that can serve the analytical optimization of experimental parameters. The target of using the response surface approach in the present study is to make statistical projections by fitting a polynomial equation to experimental data. This methodology consists of a number of mathematical and statistical

procedures that must outline the behavior of a data set. It works well when an answer or a group of relevant replies are affected by a number of different factors. To achieve the greatest system performance, it is necessary to simultaneously optimize the levels of these variables [Chelladurai et al., 2020; Sarabia et al., 2020].

In the present work, the electrodeposition technique was utilized to prepare a Mn-Ni-Co oxide electrode with different concentrations (0.05, 0.1, and 0.15) M at a constant current density of 25 mA/cm² which was chosen based on our previous study [Ahmed and Salman, 2023]. The effect of these different concentrations of salts on the specifications of prepared electrodes will be studied. The performance of composite electrodes was established through the optimization of indirect electro-oxidation technique using RSM. The major goal was to maximize elimination responses in order to achieve a rapid removal rate of COD. A series of experiments including variables like current density, pH, and NaCl content were accomplished to achieve this. Any reaction that is influenced by the values of one or more statistical variables can be modeled or optimized using the same methods. Polynomial regression modeling serves as the method's statistical basis. The operating conditions were optimized through the surface responses approach with the aid of the Analysis of Variance (ANOVA). Implementing electrochemical oxidation methods with optimized parameters in a way just like in the current study is consistent with the inclination of electrifying water treatment. It also enables a practical route for developing sustainable and environmentally friendly pathways of wastewater remediation technologies.

EXPERIMENTAL WORK

Preparation of composite electrode

Electrochemical deposition was used to create the composite electrodes with various Metallic salts, i.e., Cobalt Nitrate, Nickel Nitrate, and Manganese Chloride of different concentrations (0.05, 0.1, and 0.15 M) with a molar ratio of 1:1:1 at constant current density 25 mA/cm² within 2 hours of electrolysis.

The electrodeposition cell consisted of two flat sheets of graphite (as shown in Figure 1), each having the same dimensions (12×5×1 cm)

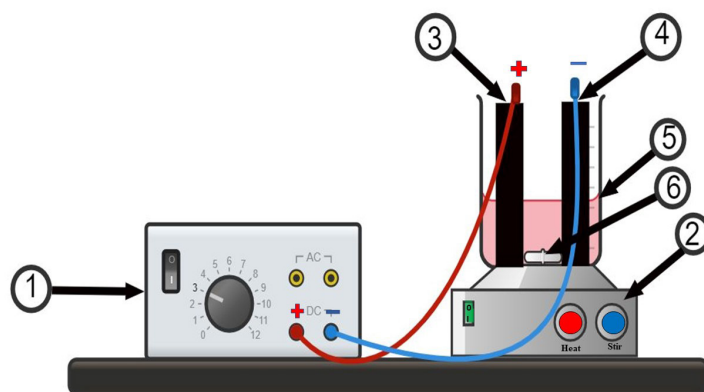


Figure 1. Electrodeposition cell schematic diagram: 1 – hot plate magnetic stirrer, 2) electrodeposition bath, 3 – cathode electrode, 4 – anode electrode, 5 – DC power supply

and utilized as anode and cathode respectively. After activating the graphite at 350 °C for 30 minutes, a better adhesion between particles and graphite was achieved [Ahmed and Salman, 2023]. Acetone was used to remove impurities on graphite electrodes prior to each experiment. This was followed by a distilled water rinse.

The sheets of graphite have been placed vertically leaving a 3 cm gap between them in a deposition bath of 0.6 L with a working area of 25 cm². The electrochemical deposition was carried out galvanostatically at 25 mA/cm² for 2 hours using a DC power supply (MS-605D, China). The prepared electrodes were washed with distilled water and then dried at air temperature.

Phenol removal

The efficiency of composite electrodes in removing phenol through indirect electrooxidation was examined. The tests were done using different amounts of electric current densities (40, 60, and 80 mA/cm²), acidity levels (3, 4, and 5), and amounts of NaCl (1, 1.5, and 2 g/l). The phenol solution is obtained by dissolving 150 mg/l of phenol (equal to 320 mg/l of COD) in aqueous solution and pH was adjusted with 0.1 M H₂SO₄ and 0.1 NaOH. In the remediation cell, there were two distinct electrodes: one was the composite electrode, commonly utilized as the anode, and the other was the graphite electrode, utilized as the cathode. These electrodes were placed vertically in the aqueous solution with 3 cm apart. The remediation process acquired 1 hour and the removal experiments were completed at normal room temperature. To determine the precise amount of phenol and any other organic by-products that might be created during the indirect oxidation process,

COD was measured for each experiment and the COD removal efficiency was described as follows [Asaithambi et al., 2020].

$$COD\ Removal\ \% = \frac{COD_o - COD_f}{COD_o} \times 100 \quad (1)$$

where: COD_o (mg/l) and COD_f (mg/l) are the initial and final values of the COD, respectively.

For the purpose of characterizing COD, samples were subjected to the recognized colorimetric approach via Lovibond water testing, Photometer- System MD200.

Equation (2) provides an estimate of the energy consumption (EC) in (kWh/kg COD) [Doumbi et al., 2022].

$$EC = \frac{I \times E \times t \times 1000}{\Delta COD \times V} \quad (2)$$

where: I is the operating current density (mA/cm²), V is the volume of the solution (L), t is the electrolysis time (h), and ΔCOD is the difference between COD_i and COD_f in mg/l.

Experimental design

Response surface methods (RSM) are multi-variable techniques that is mathematically suitable for the experimental domain investigated in the theoretical layout through a response function. The central composite and Box-Behnken designs are the two commonly used designs utilized in

response surface modeling [Panwar et al., 2020; Demirel et al., 2022]. In the present work, the RSM analysis has been used to investigate the COD removal model and determine its optimum operating parameters. The Central Composite Design (CCD) of RSM was used to examine how the response function and the variables relate to one another with a two-level full-factorial. Table 1 illustrates the ranges as well as levels of these parameters. Following multiple regression techniques, the experimental results of the COD removal were fitted with the following second-order polynomial equation.

$$Y = b_0 + b_1X_1 + b_2X_2 + b_3X_3 + b_{12}X_1X_2 + b_{13}X_1X_3 + b_{23}X_2X_3 + b_{11}X_1^2 + b_{22}X_2^2 + b_{33}X_3^2 \quad (3)$$

where: Y denotes the anticipated response (COD removal %),
 b denotes a constant,
 b₁, b₂, and b₃ denote linear coefficients,
 b₁₂, b₁₃, and b₂₃ denote cross-product coefficients,
 b₁₁, b₂₂, and b₃₃ denote quadratic coefficients and
 X₁, X₂, and X₃ are the operating variables.

RESULTS AND DISCUSSIONS

Characterization of prepared composite electrodes

Due to their versatility, electrodeposition processes can be used to produce surfaces with a variety of crystalline variants. These surfaces could form as porous deposits, high-rough deposits, uniformly dense layers, or nanostructured substances [Atta et al., 2016]. To identify the characterization of the electrodes that were created at varied metal salt concentrations, the anode-deposited electrodes are denoted as A1, B1, and C1, respectively, and the related cathode electrodes as A2, B2, and C2, respectively.

XRD analysis

X-Ray diffraction is employed to investigate the crystallization and crystalline phases of the deposition film. The patterns of MnCo₂O₄, Co₃O₄, NiO, and MnO₂ deposited on graphite electrodes are displayed in Figure 2.

Both on anode and cathode, it can be recognized that these metal composites were composed of mixed oxides containing the cubic phase of NiO (JCPDS- 47–1049), the spinal crystal of Co₃O₄ (JCPDS- 42–1467), the cubic crystal of MnO₂ (JCPDS -42–1169), and cubic spinel structure of MnCo₂O₄ (JCPDS-023–1237). There is also a modest peak observable for the cubic crystal of graphite (JCPDS- 006–0675). By comparing the other patterns of cobalt, nickel, and manganese oxide onto graphite substrate, there is only one difference in composite films of the cathode where peaks of the cubic phase of Mn₂O₃ (JCPDS card no. 41–1442) are observed.

SEM and EDX analysis

SEM was used to examine the morphology of the various synthesized samples; SEM images of the Mn-Co-Ni films on graphite substrate are shown in Figure 3. As the concentration of the Mn, Co, and Ni ions increases, the electrode materials exhibited nanosheets architectures and transitioned Nano flowers that are spherical to porous flat sheets. The electrode nanosheets are interconnected with one another. As the precursor concentration of Mn, Co, and Ni increased, the nanosheets' thickness and length varied, indicating that the net amount of the oxidized metal had grown. At low concentrations of Mn-Co-Ni (0.05 M), small spherical crystals are dispersed randomly on the surface. However, by increasing the concentration of Mn-Co-Ni to 0.15 M, the intensity of crystallites increased and this agrees with a previous study [El Boraei and Ibrahim, 2019].

The anode materials (Figure 3 A1, B1, and C1) had different morphology from the cathode materials (Figure 3 A2, B2, and C2). The anode

Table 1. Variables and their levels of experimental design

Independent variable	Levels		
	-1	0	1
X1, Current density, mA/cm ²	40	60	80
X2, pH	3	4	5
X3, NaCl conc., g/l	1	1.5	2

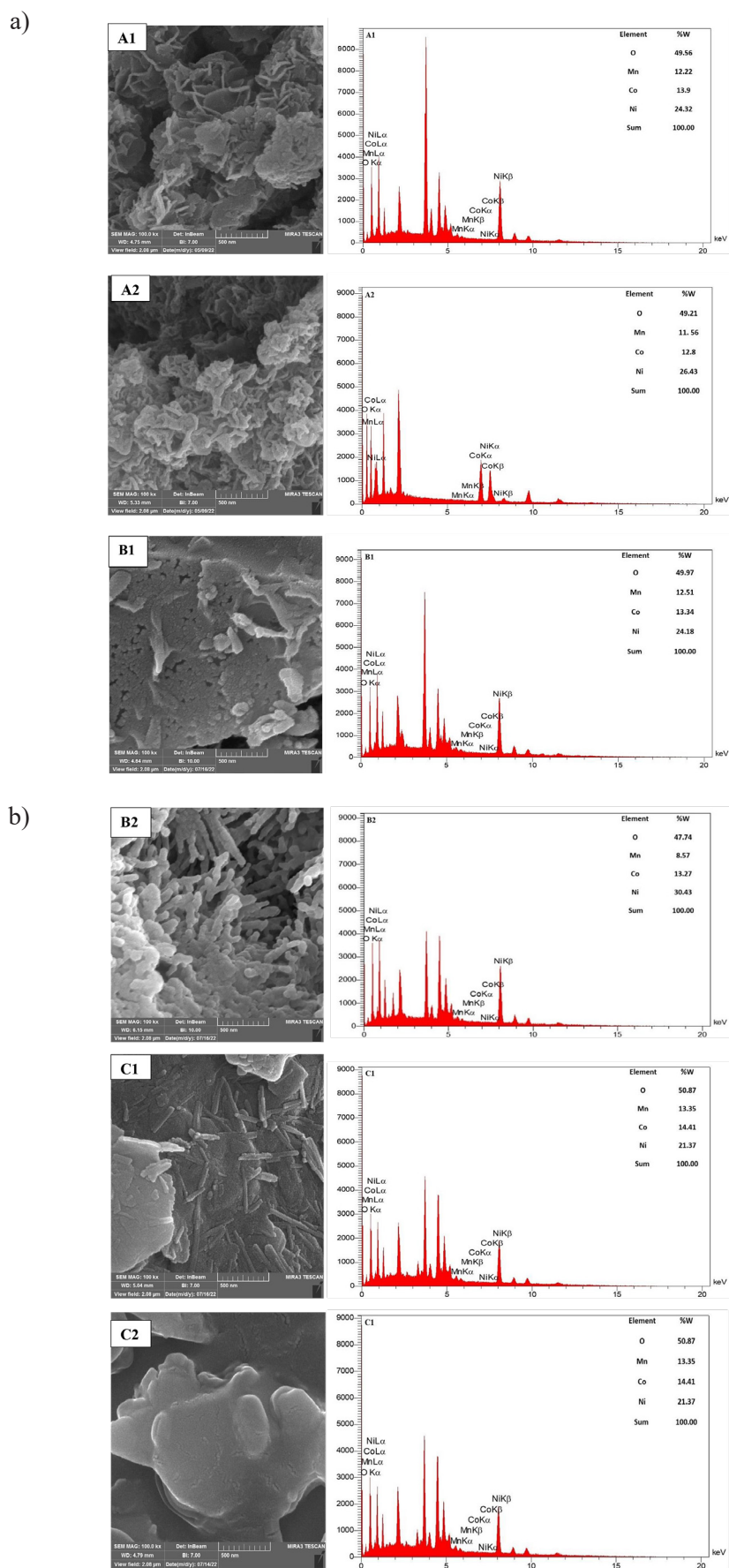


Figure 3. SEM images of (Mn-Co-Ni) oxide at magnification (500 nm) and EDX images at the anode (A1, B1, C1) and the cathode (A2, B2, C2) synthesized at different concentrations (0.05, 0.01, 0.15) M with constant molar ratio (1:1:1) at CD of 25 mA/cm² and 2 h of electrolysis

Table 2. Root mean square (Sq) of anode and cathode of manganese-cobalt-nickel oxides at different concentrations (0.05, 0.1 and 0.15) M with constant CD of 25 mA/cm² and 2 h of electrolysis

Mn- Co- Ni Concentration (M) with molar ratio (1:1:1)	Root mean square (Sq), nm	
	Anode	Cathode
0.05	66.34	128.3
0.1	23.32	88.34
0.15	7.342	44.14

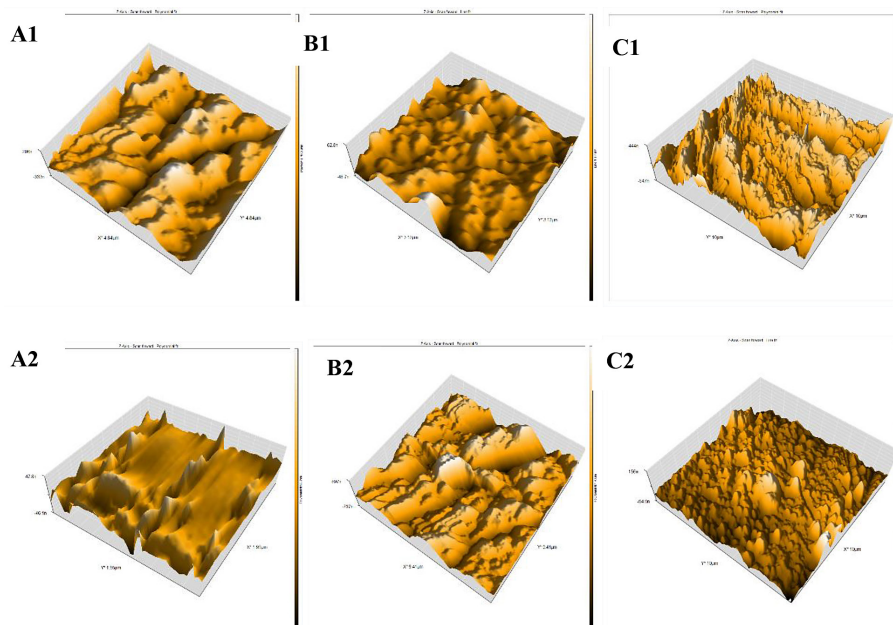


Figure 4. AFM images for manganese -cobalt -nickel oxide for the anode (A1, B1 and C1), and cathode (A2, B2, and C2) at different concentrations (0.05, 0.1, and 0.15 M) with constant molar ratio (1:1:1) at CD of 25 mA/cm² and 2 h of electrolysis

or cathode that were prepared under different concentrations are shown in Table 3. The results show that during 1 hour of electrolysis, both prepared anodes and cathodes were very effective in removing phenol and any other organic by-products. Consequently, based on these results, the anode and the cathode that were prepared with 0.05 M of Mn-Co-Ni salts under 25 mA/cm² and 2 h of electrolysis would be chosen as the anode in the process of indirect oxidation of phenol.

Statistical analysis

Development of regression model

Table 4 illustrates the actual and predicted COD removal efficiency and energy consumption that was achieved after 1 h of electrolysis. The elimination efficiency of COD was ranged from 78.078 to 100%, and the energy consumption ranged from 64.67 to 309.152 kWh/kg COD. Eq. (4) represents the regression model equations that was acquired by the MINITAB-18 software.

Table 3. COD elimination efficiency by utilizing each prepared anode or cathode as anode in indirect oxidation process

Mn- Co- Ni Concentration (M) with molar ratio (1:1:1)	COD removal % at CD = 80 mA/cm ² , pH = 3, and NaCl = 1.5 g/l	
	Anode	Cathode
0.05 M	99.92	99.94
0.1 M	99.56	99.59
0.15M	99.45	99.47

Table 4. Experimental and predicted values for COD removal% and EC

Run	Current density, X1, mA/cm ²	pH, X2	NaCl, X3, g/l	Actual COD removal %	Predicted COD removal %	EC, kWh/kg COD
1	60	4	1.5	93.400	93.687	178.44
2	60	4	1.5	93.700	93.687	194.812
3	80	3	1.0	96.526	96.068	309.152
4	60	5	1.5	92.490	91.701	113.268
5	40	4	1.5	85.610	84.803	96.722
6	40	3	1.0	81.700	81.693	177.446
7	80	5	2.0	94.165	94.436	218.01
8	60	4	2.0	95.790	94.064	151.621
9	80	5	1.0	88.510	88.494	272.590
10	60	4	1.5	92.910	93.687	205.011
11	40	5	2.0	84.035	84.757	91.609
12	60	4	1.5	93.520	93.687	224.890
13	60	4	1.5	93.590	93.687	186.710
14	80	3	2.0	100.000	100.453	152.380
15	80	4	1.5	97.080	96.830	188.030
16	60	3	1.5	96.880	96.611	141.313
17	40	3	2.0	86.723	87.003	64.67
18	60	4	1.5	92.890	93.687	179.423
19	40	5	1.0	78.078	77.890	105.37
20	60	4	1.0	87.770	88.438	200.74

$$\begin{aligned}
 \text{COD Removal \%} = & 26.94 + 1.396 X1 - 4.26 X2 + \\
 & + 33.56 X3 - 0.00727 X1^2 + 0.434 X2^2 - \quad (4) \\
 & - 9.89 X3^2 - 0.0471 X1 * X2 - \\
 & - 0.0231 X1 * X3 + 0.779 X2 * X3
 \end{aligned}$$

Analysis of variance (ANOVA)

The ratio of mean square variation resulting from regression to mean square residual error was statistically investigated via ANOVA. ANOVA was attained by the MINITAB-18 software. The response model’s regression coefficients, as well as the F and P values for COD elimination efficiencies, are shown in Table 5. Moreover, a greater F-value (> 4) seems to imply that the regression equation can largely explain the variation in the response, which is consistent with the higher F-value. The model is considered as statistically significant if the p-value is less than 0.05 [Srivastava et al., 2017]. To ascertain whether it is significant enough to demonstrate statistical significance, the associated F-value is assessed. The F and P values were 102.49 and 0.000 respectively as shown in Table 5 which emphasize the statistical significance of the model for COD Removal%.

The results showed that the second-order polynomial models (Eq. 4) were highly significant and well-fit to the experimental findings. COD removal efficiency yields an adjusted R² value of 97.96% and a coefficient of determination R² value of 98.93%. This suggested that the model offered had an appropriate approximation to the real value. The ANOVA results showed that the current density is responsible for 88.40% of the effect on COD elimination efficiency. This means that current density is the most important factor in determining how well COD is eliminated. NaCl has the second largest effect with a contribution of 12.78%, and pH contributes with 9.73%.

3mpact of parameters on the COD remediation

Figure 5 shows the 3D surface and contour plots and demonstrates how the amount of electric current density impacts the ability to remove COD. Figure 5a shows that when the current density is increased to more than 60 mA/cm² and the concentration of NaCl increases from 1.5 to 2 g/l, a high percentage (greater than 96%) of COD removal is obtained. Based on the contour plot (Figure 5b), the highest COD removal% can be obtained when the current density ranged from 70 to 80 mA/cm² and salt concentration range

Table 5. ANOVA results for removing COD by indirect electro-oxidation process

Source	DF	Seq. SS	Contribution	Adj. SS	Adj. MS	F-Value	P-Value
Model	9	612.590	98.93%	612.590	68.066	102.49	0.000
Linear	3	501.021	80.91%	501.021	167.007	251.47	0.000
Current density	1	361.622	58.40%	361.622	361.622	544.52	0.000
pH	1	60.275	9.73%	60.275	60.275	90.76	0.000
NaCl	1	79.124	12.78%	79.124	79.124	119.14	0.000
Square	3	102.819	16.60%	102.819	34.273	51.61	0.000
Current density×current density	1	85.245	13.77%	23.229	23.229	34.98	0.000
pH×pH	1	0.778	0.13%	0.517	0.517	0.78	0.398
NaCl×NaCl	1	16.796	2.71%	16.796	16.796	25.29	0.001
2-Way Interaction	3	8.750	1.41%	8.750	2.917	4.39	0.032
Current density×pH	1	7.108	1.15%	7.108	7.108	10.70	0.008
Current density×NaCl	1	0.428	0.07%	0.428	0.428	0.64	0.441
pH×NaCl	1	1.213	0.20%	1.213	1.213	1.83	0.206
Error	10	6.641	1.07%	6.641	0.664		
Lack-of-Fit	5	6.183	1.00%	6.183	1.237	13.49	0.006
Pure Error	5	0.458	0.07%	0.458	0.092		
Total	19	619.231	100.00%				

Model summary				
S	R-sq	– R-sq(adj.)	PRESS	R-sq(pred.)
0.814934	98.93%	97.96%	44.2906	92.85%

from 1.4 to 2 g/l. This is caused by an increase in the production of substances that cause oxidation, specifically hypochlorous acid (HOCl). This agrees with what other studies had found [Särkkä et al., 2015; Oliveira et al., 2018].

The impact of pH and current density on COD elimination% at constant NaCl concentration of 1.5 g/l is shown in Figure 6. In the 3D surface plot shown (Figure 6a), the COD removal efficiency increases as pH decreases from 5 to 3 (be more acidic) and as the current density increases from 40 to 80 mA/cm² due to hypochlorous acid (HOCl) generation which is the primary oxidizing

agent with larger redox potential in an acidic environment than an alkaline one [Tasic et al., 2014; Ahmed and Salman, 2023]. In the contour plot (Figure 6b), the highest COD removal efficiency achieved at pH = 3 and at a current density range from 73 to 80 mA/cm².

The impact of NaCl concentration and pH on COD elimination % at a constant current density of 60 mA/cm² is shown in Figure 7. The 3D surface plot in Figure 7a shows that the COD removal efficiency increases sharply when NaCl concentration increases from 1 to 2 g/l, and with pH decreasing from 5 to 3 due

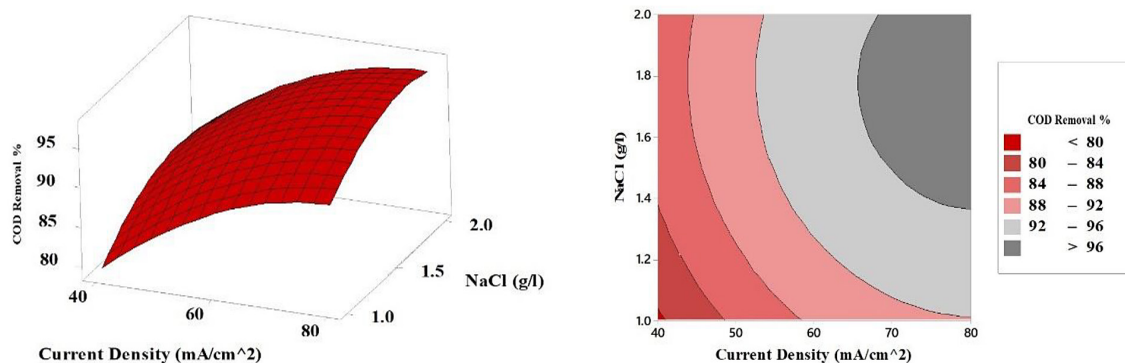


Figure 5. The impact of current density and NaCl concentration on COD removal % at pH = 4, (a) 3D surface plot, and (b) contour plot

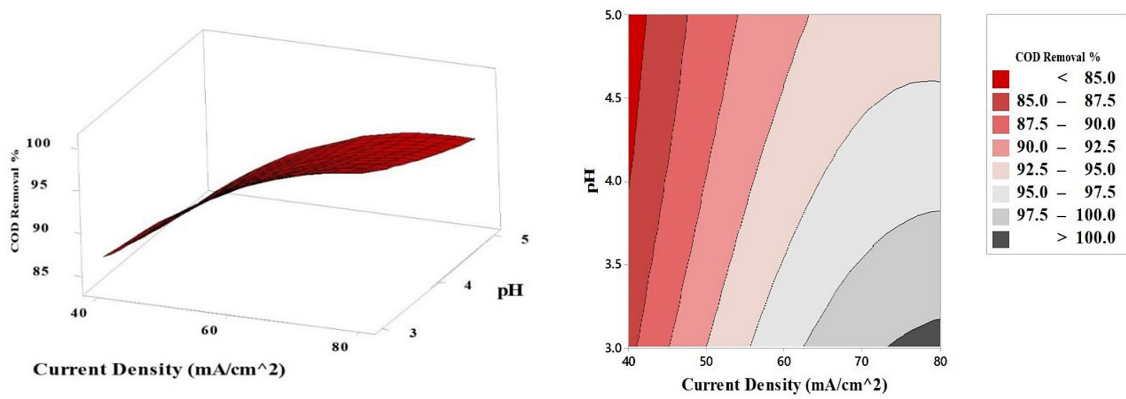


Figure 6. The impact of pH and current density on COD elimination % at NaCl concentration = 1.5 g/l, (a) 3D surface plot, and (b) contour plot

to the high influence of HOCl in acidic medium. It is consistent with earlier research that the elimination efficiency of COD increased when NaCl content increased [Periyasamy and Muthuchamy, 2018]. The highest COD elimination efficiency (> 96 %) is achieved when NaCl concentration increases from 1.5 to 2 g/l at pH = 3 and the current density 60 mA/cm² as shown in the contour plot (Figure 7b).

According to the results in Table 4, energy consumption decreased from 141.313 to 113.268 kWh/kg COD when pH increased from 3 to 5 at a current density of 60 mA/cm² and NaCl of 1.5 g/l. Furthermore, the energy consumption increased from 96.722 to 188.03 kWh/kg COD when the current density increases from 40 to 80 mA/cm² at NaCl of 1.5 g/l, and pH of 4, and decreased from 200.74 to 151.621 kWh/kg COD when NaCl concentration increased from 1 to 2 g/l at current density of 60 mA/cm², and pH of 4.

The optimization and confirmation test

The optimization of process variables has been suggested in the study of any electrochemical removal system to reduce energy losses and, as a result, the expense of treatment losses. Criteria must be exposed to the system’s optimization to achieve the goal. To do this, one must identify the precise point at which the function of desirability (DF) is maximized by controlling the weight or importance that could alter an object’s properties. The target fields’ factors were separated into five classifications: none of it, maximize, minimize, goal, and the limits of the range [Chakawa and Aziz, 2021]. In the present study, the target is set as “maximum” due to maximize COD removal%. With these parameters and limitations, optimization was carried out using the desirability function of (1), and the results are displayed in Table 6. Two experiments were accomplished based on the optimized settings as a confirmation step and Table 7 presents the results. After 1 hour

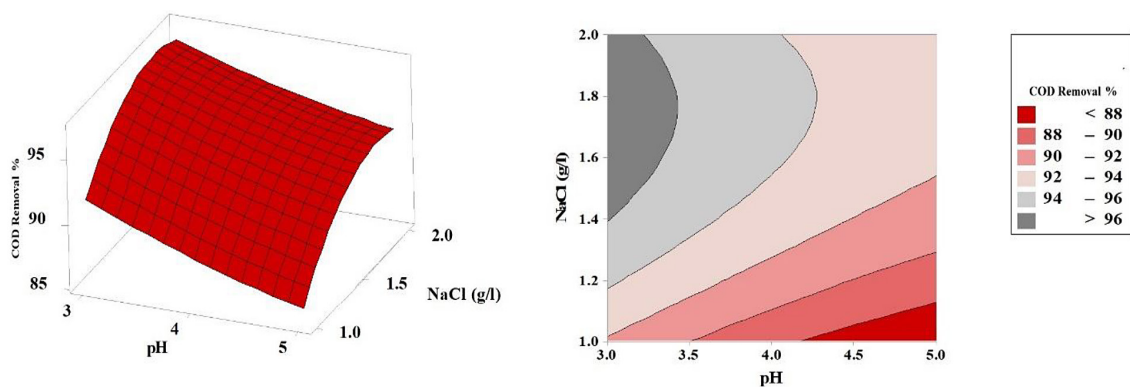


Figure 7. The impact of NaCl concentration and pH on COD elimination % at current density 60 mA/cm², (a) 3D surface plot, and (b) Contour plot

Table 6. Optimum results of the system's variables for the highest COD elimination

Response	Goal	Lower	Target	Upper	Weight	Importance	
Actual COD removal %	Maximum	78.078%	100	100	1	1	
Solution of parameters			Multiple response Prediction				
Current density, mA/cm ²	pH	NaCl conc., g/l	COD removal % Fit	SE Fit	95% CI	95% PI	Composite desirability
80	3	1.71717	101.204	0.669	(99.712; 102.695)	(98.854; 103.554)	1

Table 7. Confirmation tests for COD removal efficiency, and consumed energy

Run	Current density, mA/cm ²	pH	NaCl conc. (g/l)	E, volt	EC, kWh/kg COD	Actual COD removal %	Average
1	80	3	1.717	16	169.329	99.85	99.925%
2	80	3	1.717	14.4	152.380	100.00	

of electrolysis, the range of the maximum value was determined from maximizing the efficiency analysis with the desirability function of (1) may be compacted with the elimination efficiency of 99.925% that accomplished at current density of 80 mA/cm², pH = 3, and NaCl conc. = 1.717 g/l. Therefore, the tertiary composite electrode prepared at 0.05 M with a constant molar ratio (1:1:1) at a current density of 25 mA/cm² indicated that these electrodes are especially effective when compared to previous studies that investigated the electrochemical degradation of phenol and other organic by-products.

Abbas et al. (2016) studied the efficiency of MnO₂/graphite electrode in eliminating phenol by indirect oxidation. They found that by using this electrode, they were able to eliminate more than 95% of the phenol in 5 hours [Abbas et al., 2016]. By comparing the results of the present study with this previous study, the high efficiency of the prepared multicomponent metal oxides in removing phenol and any other organic byproducts within lower electrolysis time is a promising result.

CONCLUSIONS

The deposits of multicomponent oxides of manganese, cobalt, and nickel that formed instantaneously on the anode and cathode of the electrochemical cell were remarkably well-formed, according to the results of XRD, SEM, EDX, and AFM analyses. These metal oxides

enhanced the performance of the graphite electrodes in phenol and any other organic byproducts elimination by indirect electrochemical oxidation. The results of XRD, SEM, EDX, and AFM analyses, as well as the instantaneous removal trials for phenol showed that the electrode constructed with 0.05 M at 25 mA/cm² was the most effective electrode for eliminating COD. Both prepared anode and cathode had the same effectiveness for phenol removal by indirect electro-oxidation. RSM was a useful technique for optimizing the parameters of the indirect electro-oxidation process. The model assumed theoretical response values matched the results of the experiments. Therefore, showing the response surface models' accurateness and precision. In each test area, the second-order model accurately characterized the response. According to the Central Composite Design, the optimum operating parameters for the COD degradation were a current density of 80 mA/cm², pH of 3, and 1.1717 g/l of NaCl. Therefore, the highest rate of COD degradation was 99.925% with an energy consumption of 160.8545 kWh/kg COD. COD elimination rate improved with increasing current density and NaCl content, but decreased with increasing pH value. The prepared Mn-Co-Ni oxide electrode successfully removed phenol and other organics byproducts by indirect electro-oxidation with high removal efficiency, short electrolysis time (1 hour), and less energy consumption compared with the single oxides in previous studies.

REFERENCES

1. Abbar A. H., Alkurdi S. S. 2021. Performance evaluation of a combined electrocoagulation– electrooxidation process for the treatment of petroleum refinery wastewater. *IOP Conference Series: Materials Science and Engineering*, 1076(1), 012027.
2. Abbas A. S., Hafiz M. H., Salman R. H. 2016. Indirect electrochemical oxidation of phenol using rotating cylinder reactor. *Iraqi Journal of Chemical and Petroleum Engineering*, 17(4), 43–55.
3. Abbas R. N., Abbas A. S. 2022. Kinetics and energetic parameters study of phenol removal from aqueous solution by electro-fenton advanced oxidation using modified electrodes with PbO₂ and graphene. *Iraqi Journal of Chemical and Petroleum Engineering*, 23(2), 1–8.
4. Abbas Z. I., Abbas A. S. 2019. Oxidative degradation of phenolic wastewater by electro-fenton process using MnO₂-graphite electrode. *Journal of Environmental Chemical Engineering*, 7(3).
5. Abebe E. M., Ujihara M. 2022. Simultaneous electrodeposition of ternary metal oxide nanocomposites for high-efficiency supercapacitor applications. *ACS Omega*, 7(20), 17161–17174.
6. Adil Sabbar H. 2019. Adsorption of phenol from aqueous solution using paper waste. *Iraqi Journal of Chemical and Petroleum Engineering*, 20(1), 23–29.
7. Ahmed Y. A., Salman R. H. 2023. Simultaneous electrodeposition of multicomponent of Mn–Co–Ni oxides electrodes for phenol removal by anodic oxidation. *Case Studies in Chemical and Environmental Engineering*, 8.
8. Al-Yaqoobi A.M., Al-Rikabey M.N., Algharrawi K.H.R. 2021. Treatment of dairy wastewater by electrocoagulation and ultrasonic-assisted electrocoagulation methods. *Environmental Engineering & Management Journal*, 20(6), 949–957.
9. Asaithambi P., Govindarajan R., Yesuf M. B., Alemayehu E. 2020. Removal of color, COD and determination of power consumption from landfill leachate wastewater using an electrochemical advanced oxidation processes. *Separation and Purification Technology*, 233.
10. Atta N. F., El-Ads E. H., Galal A. 2016. Self-assembled monolayers on nanostructured composites for electrochemical sensing applications. *Handbook of Nanoelectrochemistry: Electrochemical Synthesis Methods, Properties, and Characterization Techniques* (417–478), Springer International Publishing.
11. Chakawa S., Aziz M. 2021. Investigating the result of current density, temperature, and electrolyte concentration on cod: Subtraction of petroleum refinery wastewater using response surface methodology. *Water (Switzerland)*, 13(6).
12. Chelladurai S. J. S., Murugan K., Ray A. P., Upadhyaya M., Narasimharaj V., Gnanasekaran S. 2020. Optimization of process parameters using response surface methodology: A review. *Materials Today: Proceedings*, 37, 1301–1304.
13. Cysewska K., Rybarczyk M. K., Cempura G., Karczewski J., Łapiński M., Jasinski P., Molin S. 2020. The influence of the electrodeposition parameters on the properties of Mn-Co-based nanofilms as anode materials for alkaline electrolyzers. *Materials*, 13(11).
14. Demirel C., Kabutey A., Herák D., Sedláček A., Mizera Č., Dajbych O. 2022. Using Box–Behnken Design Coupled with Response Surface Methodology for Optimizing Rapeseed Oil Expression Parameters under Heating and Freezing Conditions. *Processes*, 10(3).
15. Doumbi R. T., Bertrand Noumi G., Ngobtchok B., Domga. 2022. Tannery wastewater treatment by electro-Fenton and electro-persulfate processes using graphite from used batteries as free-cost electrode materials. *Case Studies in Chemical and Environmental Engineering*, 5.
16. El Boraie N. F., Ibrahim M. A. M. 2019. Black binary nickel cobalt oxide nano-powder prepared by cathodic electrodeposition; characterization and its efficient application on removing the Remazol Red textile dye from aqueous solution. *Materials Chemistry and Physics*, 238.
17. Jadhav S. M., Kalubarme R. S., Suzuki N., Terashima C., Mun J., Kale B. B., Gosavi S. W., Fujishima A. 2021. Cobalt-Doped Manganese Dioxide Hierarchical Nanostructures for Enhancing Pseudocapacitive Properties. *ACS Omega*, 6(8), 5717–5729.
18. Jiráťová K., Perekrestov R., Dvořáková M., Balabánová J., Koštejn M., Veselý M., Čada M., Topka P., Pokorná D., Hubička Z., Kovanda F. 2021. Modification of cobalt oxide electrochemically deposited on stainless steel meshes with Co-Mn thin films prepared by magnetron sputtering: Effect of preparation method and application to ethanol oxidation. *Catalysts*, 11(12).
19. Li M., Cheng J. P., Wang J., Liu F., Zhang X. B. 2016. The growth of nickel-manganese and cobalt-manganese layered double hydroxides on reduced graphene oxide for supercapacitor. *Electrochimica Acta*, 206, 108–115.
20. Ibrahim H. M., Salman R. H. 2022. Study the Optimization of Petroleum Refinery Wastewater Treatment by Successive Electrocoagulation and Electro-oxidation Systems. *Iraqi Journal of Chemical and Petroleum Engineering*, 23(1), 31–41.
21. Massa A., Hernández S., Lamberti A., Galletti C., Russo N., Fino D. 2017. Electro-oxidation of phenol over electrodeposited MnOx nanostructures and the role of a TiO₂ nanotubes interlayer. *Applied Catalysis B: Environmental*, 203, 270–281.
22. Nady H., El-Rabiei M. M., El-Hafez G. M. A. 2017.

- Electrochemical oxidation behavior of some hazardous phenolic compounds in acidic solution. *Egyptian Journal of Petroleum*, 26(3), 669–678.
23. Oliveira E. M. S., Silva F. R., Morais C. C. O., Oliveira T. M. B. F., Martínez-Huitle C. A., Motheo A. J., Albuquerque C. C., Castro S. S. L. 2018. Performance of (in)active anodic materials for the electrooxidation of phenolic wastewaters from cashew-nut processing industry. *Chemosphere*, 201, 740–748.
 24. Panwar V., Kumar Sharma D., Pradeep Kumar K. V., Jain A., Thakar C. 2020. Experimental investigations and optimization of surface roughness in turning of en 36 alloy steel using response surface methodology and genetic algorithm. *Materials Today: Proceedings*, 46, 6474–6481.
 25. Periyasamy S., Muthuchamy M. 2018. Electrochemical oxidation of paracetamol in water by graphite anode: Effect of pH, electrolyte concentration and current density. *Journal of Environmental Chemical Engineering*, 6(6), 7358–7367.
 26. Sarabia L. A., Ortiz M. C., Sánchez M. S. 2020. Response Surface Methodology. *Comprehensive Chemometrics*, 287–326.
 27. Särkkä H., Bhatnagar A., Sillanpää M. 2015. Recent developments of electro-oxidation in water treatment—A review. *Journal of Electroanalytical Chemistry*.
 28. Sayyed S. G., Mahadik M. A., Shaikh A. V, Jang J. S., Pathan H. M. 2019. Nano-metal oxide based supercapacitor via electrochemical deposition. *ES Energy & Environment*.
 29. Srivastava M., Maheshwari S., Kundra T., Rathee S. 2017. Multi-response optimization of fused deposition modelling process parameters of ABS using response surface methodology (RSM)-based desirability analysis. *Materials Today: Proceedings*, 4, 1972–1977.
 30. Sui Q., Xiang C., Zou Y., Yan E., Zhang H., Xu F., Sun L. 2019. Facile synthesis of Co-Ni-Mn oxide for high performance supercapacitor. *International Journal of Electrochemical Science*, 14, 10710–10719.
 31. Tahmasebi M. H., Vincenzo A., Hashempour M., Bestetti M., Golozar M. A., Raeissi K. 2016. Nanosized Mn-Ni oxide thin films via anodic electrodeposition: A study of the correlations between morphology, structure and capacitive behaviour. *Electrochimica Acta*, 206, 143–154.
 32. Tasic Z., Gupta V. K., Antonijevic M. M. 2014. The Mechanism and kinetics of degradation of phenolics in wastewaters using electrochemical oxidation. *Int. J. Electrochem. Sci.*, 9.
 33. Tegua Doumbi R., Noumi G. B., Domga. 2021. Dip coating deposition of manganese oxide nanoparticles on graphite by sol gel technique for the indirect electrochemical oxidation of methyl orange dye: Parameter's optimization using box-behnken design. *Case Studies in Chemical and Environmental Engineering*, 3.
 34. Yan Z., Liu H., Hao Z., Yu M., Chen X., Chen J. 2020. Electrodeposition of (hydro)oxides for an oxygen evolution electrode. *Chemical Science*. Royal Society of Chemistry.
 35. Zhu K., Qi H., Sun X., Sun Z. 2019. Anodic oxidation of diuron using Co_3O_4 /graphite composite electrode at low applied current. *Electrochimica Acta*, 299, 853–862.